Radiationless Deactivation of Singlet Oxygen ($^1\Delta_g$) by Solvent Molecules†

R. Schmidt* and H.-D. Brauer

Contribution from the Institut für Physikalische Chemie, Universität Frankfurt, Niederurseler Hang, D6000 Frankfurt/Main, FRG. *Received March 16, 1987*

Abstract: A very sensitive infrared emission spectrometer was used to determine $^1O_2$ lifetimes (τ_Δ) by following directly the decay of $O_2(^1\Delta_g, v = 0) \rightarrow (^3\Sigma_g^-, v = 0)$ emission at 1270 nm. Use of excitation pulses of about 10^3 times smaller energy and of about 10^9 times weaker power than in previous laser pulse experiments allowed observation of much longer lifetimes in several perhalogenated solvents, CS_2, and $CDCl_3$. A maximum value of $\tau_\Delta = 99$ ms was found for Freon 113. Thus τ_Δ varies from 4 to 100 000 μs, depending on solvent. Incremental rate constants k_{XY} of energy transfer from $^1O_2$ to terminal oscillators X–Y contained in the solvent molecules were calculated to understand the strong effect of solvent on $^1O_2$ lifetime. A strong exponential correlation was found between k_{XY} and the highest fundamental energy E_{XY} of oscillator X–Y. A collisional $E \rightarrow V + R + T$ energy transfer describing quantitatively the dependence of k_{XY} on E_{XY} and of τ_Δ on solvent is discussed.

Since the first direct observation of singlet oxygen ($^1\Delta_g$, $v = 0) \rightarrow (^3\Sigma_g^-, v = 0)$ emission in solution at 1270 nm by Krasnovsky,[1] lifetime (τ_Δ) determinations of singlet oxygen ($^1O_2$) have been performed in several laboratories using the direct spectroscopic observation method.[2-13] A strong solvent effect on τ_Δ was observed. τ_Δ values obtained by different methods (i.e., time-resolved flash or laser pulse experiments, phosphoroscope measurements, or steady-state emission spectroscopy) agreed rather well in the time domain below about 700 μs. However, for longer lifetimes different methods resulted in very different τ_Δ values, scattering at maximum by a factor of 40.[1,4,5,8,9,12] It was recognized that in those crucial solvents (i.e., halogenated solvents and CS_2) τ_Δ increases with decreasing intensity of the exciting radiation.[5,7,9,11,12]

Since we now are able to measure directly $^1O_2$ lifetimes (if $\tau_\Delta \geq 7$ ms) using excitation pulses of about 10^3 times smaller energy and of about 10^9 times weaker power than in the previous laser pulse experiments[5-7,11-13] (excitation intensities are several orders of magnitude smaller than in the phosphoroscope and steady-state emission experiments[1,8]), we presumed that we could measure the real $^1O_2$ lifetimes in perhalogenated solvents and CS_2.

Deactivation of $^1O_2$ by solvents is a conversion of electronic excitation energy into vibrational energy in which the solvent molecule accepts the energy partially or even completely in the first step.

The most advanced model for interpreting the solvent dependence of τ_Δ values was developed by Schuster et al.[12] These authors separated the second-order $^1O_2$ deactivation rate constants into increments corresponding to terminal atom pairs of the solvent molecules, which serve as energy-accepting oscillators, e.g., C–H, C–D, O–H, and O–D. It was realized that for the given four oscillators X–Y the incremental rate constant of $^1O_2$ deactivation k_{XY} increases with increasing energy of the highest fundamental frequency vibration of X–Y. On the basis of this finding a qualitative explanation was given for $^1O_2$ deactivation by solvents containing the above molecular groups. However, the oscillators C–Cl, C–F, and C=S did not fit into this scheme.

Possibly this resulted from wrong τ_Δ values determined for solvents containing exclusively C–Cl, C–F, or C=S groups. In order to investigate whether a general unequivocal correlation between k_{XY} and X–Y vibrational energies exists, which finally could give a better physical understanding of the $^1O_2$ deactivation mechanism by solvent molecules, we measured $^1O_2$ lifetimes in several weakly deactivating solvents.

Experimental Section

The solvents used were perfluorohexane (C_6F_{14}, 99%), hexafluorobenzene (C_6F_6, 98–99%), and fluorotrichloromethane ($CFCl_3$, 99%) from Aldrich and 1,1,2-trifluorotrichloroethane ($C_2F_3Cl_3$ (Freon 113)), tetrachloromethane (CCl_4), carbon disulfide (CS_2), and deuteriochloroform ($CDCl_3$, 99.8%) from Merck (Uvasol series). All solvents except $CFCl_3$, which boils at 23.7 °C, were purified by column chromatography with neutral Al_2O_3 (Woelm). 5,10,15,20-Tetraphenylporphine (TPP) (Aldrich Gold Label) and perylene (PER) (Merck) were used without further purification. Rubicene (RUB) was prepared by the procedure described by Clar.[14] All solutions were air saturated and the experimental temperature was about 22 °C if not otherwise noted.

The excitation source of our home-built emission spectrometer consisted of a feedback-controlled high-pressure mercury arc lamp and a Kratos GM 252 grating monochromator. The illuminated area of the rectangular fluorescence cell was about 0.25 cm^2. $^1O_2$ emission was observed in a 90° arrangement through a Schott RG 1000 filter and a stepping motor driven Kratos GM 252 monochromator (IR grating, blaze 1000 nm) by a liquid N_2 cooled E0817L Ge diode (bias 250 V) (North Coast). Emission spectra could be recorded by means of a chopper, a PAR 128A lock-in amplifier, a 12-bit digitizer, and an Apple IIe microcomputer. In time-dependent experiments the diode signal was fed into an 8-bit Biomation 2805 transient recorder from which data were transferred to the microcomputer. Light pulses were produced from the continuous excitation by chopping with a modified chopper wheel running at 2.5 Hz. The only window had an aperture of 9°, effecting repeated excitation pulses of 10-ms duration. The intensity of exciting radiation striking the probe was determined by actinometry to be at maximum 2 mW cm^{-2}. Thus the incident radiation had a power of <1 mW and the pulse energy amounted to <10 μJ. The response of our Ge detector on 10-ms pulses was determined to be $\tau_r = 5.1$ ms by monitoring TPP fluorescence. Figure 2 illustrates the instrumental response to pulsed TPP fluorescence compared with $^1O_2$ emission decay. Obviously, a rather slow decay follows the first exponential decay. Experiments using different excitation intensities and fluorescing compounds revealed that the slow decay results from a decrease of dark current of the detector caused by thermal equilibration after radiative heating of the diode surface. For the evaluation of each individual emission decay the slow dark current decay was approximated by a single exponential, extrapolated, and subtracted from the experimental values in such a way that the difference was monoexponential over at least 4 half-lifetimes. The experimentally measured lifetimes τ_m are composites of $^1O_2$ lifetimes and the known instrumental decay time τ_r. τ_Δ values are calculated from eq 1.[10] In

$$\tau_\Delta = (\tau_m^2 - \tau_r^2)^{1/2} \quad (1)$$

temperature-dependent experiments a liquid N_2 cooled temperature-controlled cryostat DN 1704 (Oxford Instruments) was applied.

† Dedicated to Professor Albert Weller on the occasion of his 65th birthday.

(1) Krasnovsky, A. A., Jr. *Photochem. Photobiol.* **1979**, *29*, 29.
(2) Byteva, I. M.; Gurinovitch, G. P. *J. Lumin.* **1979**, *21*, 17.
(3) Kahn, A. U.; Kasha, M. *Proc. Natl. Acad. Sci. U.S.A.* **1979**, *76*, 6046.
(4) Salokhiddinov, K. I.; Dzhagarov, B. M.; Byteva, I. M.; Gurinovitch, G. P. *Chem. Phys. Lett.* **1980**, *76*, 85.
(5) Hurst, J. R.; McDonald, J. D.; Schuster, G. B. *J. Am. Chem. Soc.* **1982**, *104*, 2065.
(6) Parker, J. G.; Stanbro, W. D. *J. Am. Chem. Soc.* **1982**, *104*, 2067.
(7) Ogilby, P. R.; Foote, C. S. *J. Am. Chem. Soc.* **1982**, *104*, 2069.
(8) Jenny, T. A.; Turro, N. J. *Tetrahedron Lett.* **1982**, *23*, 2923.
(9) Stevens, B.; Marsh, K. L. *J. Phys. Chem.* **1982**, *86*, 4473.
(10) Rodgers, M. A. J. *Photochem. Photobiol.* **1983**, *37*, 99.
(11) Ogilby, P. R.; Foote, C. S. *J. Am. Chem. Soc.* **1983**, *105*, 3423.
(12) Hurst, J. R.; Schuster, G. B. *J. Am. Chem. Soc.* **1983**, *105*, 5756.
(13) Rodgers, M. A. J. *J. Am. Chem. Soc.* **1983**, *105*, 6201.
(14) Clar, E.; Willicks, W. *J. Chem. Soc.* **1958**, 942.

0002-7863/87/1509-6976$01.50/0

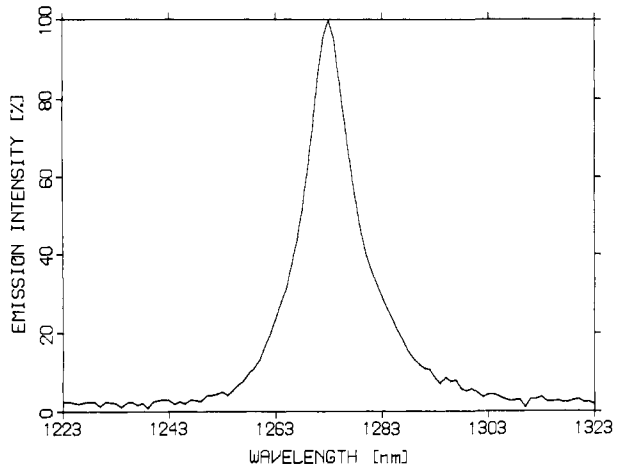

Figure 1. $O_2(^1\Delta_g, v = 0) \rightarrow (^3\Sigma_g^-, v = 0)$ emission in liquid $CFCl_3$ at −100 °C. Sensitizer [TPP] = 10^{-6} M, λ_{exc} = 405 nm. Spectral bandwidth of emission monochromator set to 1.2 nm.

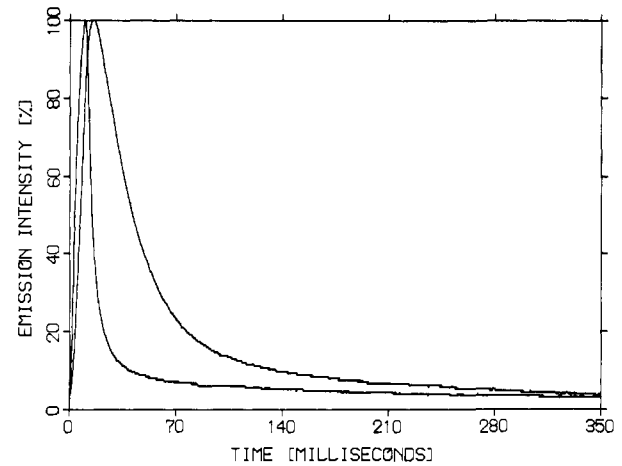

Figure 2. Time-dependent emissions. Solvent C_6F_6, sensitizer [TPP] = 10^{-6} M, λ_{exc} = 405 nm. Left decay: TPP fluorescence, λ_{em} = 720 nm. Right decay: $^1O_2$ phosphorescence, λ_{em} = 1270 nm.

Results

A. Spectra. With narrow emission monochromator slits the $O_2(^1\Delta_g, v = 0) \rightarrow (^3\Sigma_g^-, v = 1)$ emission spectra were always found to be asymmetrical. Figure 1 illustrates a spectrum, which was recorded with TPP as sensitizer in $CFCl_3$ at −100 °C. Although the spectral bandwidth of the emission monochromator was set to only 1.2 nm, no further resolution of the emission band could be achieved. Its half-bandwidth of $\lambda_{1/2}$ = 10 nm, which is about 1.6-fold narrower than at room temperature, is obviously a consequence of the system's thermal energy. Since the sensitivity of our detection system is rather wavelength independent in this wavelength region, the distinct asymmetry of the emission band is real and reflects splitting of the emission into R, Q, and P branches.

Actually a $(^1\Delta_g, v = 0) \rightarrow (^3\Sigma_g^-, v = 0)$ emission spectrum with partially resolved structure recorded by Whitlow and Findlay in the gas phase demonstrates that the high-energy R branch declines much steeper than the low-energy P branch.[15] Thus for the first time the rotational splitting of the $^1O_2$ emission at 1278 nm in liquid phase is indicated, although not being resolved.

B. $^1O_2$ Lifetimes. Figure 2 shows typical $^1O_2$ emission decay in C_6F_6 in addition to the instrumental response function, which was discussed in the Experimental Section.

1. Sensitizer Concentration Dependence. The $^1O_2$ lifetimes depend on sensitizer concentration. In Figure 3 this is demonstrated for TPP as sensitizer in CCl_4. From the slope of the straight line the rate constant of $^1O_2$ quenching by TPP is calculated to be $k_q = 7.0 \times 10^5$ M^{-1} s^{-1}. Similar experiments were done with RUB and PER in a series of solvents. It turned out that the quenching activity decreased in the series TPP > RUB > PER. The results of these experiments will be discussed elsewhere.[16]

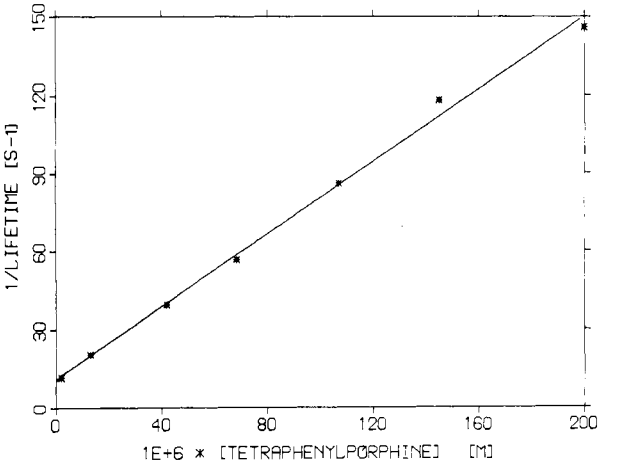

Figure 3. Dependence of $^1O_2$ deactivation rate on [TPP]. Solvent CCl_4, λ_{exc} = 405 nm, λ_{em} = 1270 nm.

Table I. $^1O_2$ Lifetimes in Various Solvents

solvent	τ_Δ, ms this work	τ_Δ, ms previous data
$C_2F_3Cl_3$	99 ± 3	18[9]
C_6F_{14}	96 ± 3	
CCl_4	87 ± 3	0.9,[5] 26[4,18]
CS_2	34 ± 1	1.5,[9] 7.4[12]
C_6F_6	25 ± 1	3.9[12]
$CFCl_3$	24 ± 1[a]	
$CDCl_3$	9.4 ± 0.5	0.64[5]

[a] Solvent was not purified by chromatography.

Since the sensitizer can act as a quencher of $^1O_2$, too, in lifetime experiments its concentration can become a crucial parameter. For example, in CCl_4 already [TPP] = 1.6×10^{-5} M is sufficient to reduce τ_Δ to 50% of its actual value. We therefore carefully avoided $^1O_2$ quenching by sensitizers by using maximum concentrations of [TPP] ≤ 10^{-6} M, [RUB] ≤ 4×10^{-6} M, and [PER] ≤ 2×10^{-6} M, depending on the kind of solvent.

2. Sensitizer Dependence. In CS_2, CCl_4, and $C_2F_3Cl_3$ we tested the three sensitizers. In CS_2 and $C_2F_3Cl_3$ we found τ_Δ to be independent of the sensitizer. With PER, having the highest S_1 excitation energy, however, a reduction of τ_Δ by about 60% was observed in CCl_4. Continuous irradiation further decreased τ_Δ. Therefore this effect is caused by photochemically induced quencher production, probably by solvent decomposition. Actually, Encinas et al. observed weak fluorescence quenching of PER by CCl_4.[17] To avoid photochemically induced quencher production we therefore used the low energy sensitizer TPP in the remaining solvents.

3. Excitation Wavelength Dependence. The application of a chopped mercury arc as pulsed excitation source offers the opportunity to probe the influence of excitation wavelength λ_{exc} on τ_Δ. Independent of λ_{exc} we found at 334, 365, and at 546 nm the same τ_Δ values with RUB in CCl_4.

4. Excitation Intensity Dependence. As discussed in the introduction we were able to use much lower excitation intensities than in previous investigations. In order to test whether under our conditions τ_Δ depends on excitation intensity we varied this parameter at 405 nm by a factor of 10 using TPP in C_6F_6. No effect on τ_Δ was observed.

(15) Whitlow, S. H.; Findlay, F. D. *Can. J. Chem.* **1967**, *45*, 2087.

(16) Seikel, K.; Schmidt, R.; Brauer, H.-D., to be published.

(17) Encinas, M. V.; Rubio, M. R.; Lissi, E. A. *J. Photochem.* **1982**, *18*, 137.

Table II. Second-Order Rate Constants of $^1O_2$ Deactivation in the Gas Phase (k_D^g) and in the Pure Liquid Phase (k_D^l)

quencher	k_D^g, M^{-1} s^{-1}	k_D^l, M^{-1} s^{-1}
H_2O	3400[19]	4300[13]
CH_3COCH_3	1000[20]	1500[13]
C_6H_6	3200[19]	2800[13]

5. Temperature Dependence. In earlier investigations only a negligible influence of temperature on τ_Δ was reported.[11,12] Since these studies were done with solvents of rather short $^1O_2$ lifetime, we also looked for the temperature dependence of τ_Δ. With TPP as sensitizer τ_Δ increased by 44% in CS_2 in going from 295 to 173 K. With the same sensitizer τ_Δ increased by 39% in $CDCl_3$ when the temperature was reduced from 295 to 223 K. Thus only a very weak effect on τ_Δ was found.

6. $^1O_2$ Lifetime Data. In Table I $^1O_2$ lifetimes determined by us are compared with τ_Δ values of earlier studies using the time-dependent direct spectroscopic method. Obviously, our values are much larger than previous data. This is most probably a consequence of solvent purification and reduction of excitation intensity. Thus the lifetime of $^1O_2$ depends extraordinarily on the nature of the solvent. Lifetimes range from 4 μs (H_2O) to 100 ms ($C_2F_3Cl_3$ (Freon 113)).

As a referee commented, the $^1O_2$ lifetime in air at atmospheric pressure is limited to 100 ms due to collisional deactivation by $O_2(^3\Sigma_g^-)$. On the basis of experimental findings of Stevens and Marsh,[9] who observed in O_2-saturated solutions of Freon 113 and CS_2 slightly (25% and 10%) shorter τ_Δ values than in the air-saturated case, the referee supposed that $^1O_2$ lifetimes in Freon 113, C_6F_{14}, and CCl_4 might also be limited due to quenching by O_2. However, Stevens and Marsh observed much shorter (5–20 times) τ_Δ values than we did, as shown in Table I. This probably resulted from photochemically induced impurity quenching caused by the intense and polychromatic radiation of a photoflash used for excitation. Since wrong $^1O_2$ lifetimes had been obtained the supposed O_2 concentration dependence of course is doubtful.

As shown in the next section, rate constants of collisional quenching of $^1O_2$ are the same in the gas phase and in the liquid phase. Since the O_2 concentration at room temperature is on the average 5 times smaller in air-saturated organic liquids than in air at 1 bar, a limiting value of τ_Δ due to quenching by O_2 should be about 500 ms in solution. As this estimate is much larger than the experimentally determined lifetimes of Table I, collisional deactivation of $^1O_2$ by $O_2(^3\Sigma_g^-)$ can be ruled out to play an important role.

This conclusion is supported by preliminary experiments which we performed. Independently of whether the solution was air saturated or O_2 saturated we measured the same τ_Δ values with RUB as sensitizer in CS_2.

Discussion

The radiationless deactivation of $^1O_2$ in the liquid phase is definitely a bimolecular energy-transfer process between $^1O_2$ and solvent molecules. This is demonstrated by the accordance of second-order rate constants of $^1O_2$ quenching by solvent molecules determined by completely different methods in the dilute gas phase and in the pure liquid phase. Table II lists these values, which have been taken from the literature.

The solvent effect on τ_Δ was first interpreted by Merkel and Kearns.[21] They proposed $^1O_2$ deactivation by electronic to vibrational (E → V) energy transfer from $^1O_2$ to solvent molecules following a mechanism similar to Försters's electric dipole resonant electronic energy transfer. Consequently the strength of solvent absorption resonant with the $(^1\Delta_g, v = 0) \rightarrow (^3\Sigma_g^-, v = 0)$ and $^1\Delta_g, v = 0) \rightarrow (^3\Sigma_g^-, v = 1)$ transitions of O_2 at 7880 and 6330 cm^{-1} should correlate with the rate constants of $^1O_2$ deactivation.

Meanwhile a large number of reliable lifetimes have been determined. However, τ_Δ values correlate only qualitatively with the above-mentioned optical solvent properties.[11,12] Foote et al.[11] and Salokhiddinov et al.[22] tried to improve Merkel and Kearn's relation. But these modifications also could not quantitatively describe experimentally determined τ_Δ values.[5]

At the same time Schuster et al. and Rodgers found that second-order rate constants k_D of $^1O_2$ deactivation by strongly deactivating solvents containing terminal X–Y atom pairs (X–Y = C–H, C–D, O–H, and O–D) are, to a good approximation, composed additively from incremental rate constants k_{XY}.[12,13] Using eq 2, with [S] the molar concentration of the solvent and

$$(\tau_\Delta[S])^{-1} = k_D = \sum_{XY} N_{XY} k_{XX} \quad (2)$$

N_{XY} the number of times a particular X–Y pair occurs per molecule, it is possible to calculate from k_{XY} values $^1O_2$ lifetimes that are in reasonable agreement with experimental data.[12] Using slightly different increments, Rodgers demonstrated the accuracy of this method for a large number of solvents.[13]

By comparing the plot of $1/\tau_\Delta$ values for a series of C–H-containing solvents against Kearn's optical density parameters with the plot of $1/\tau_\Delta$ against the molar concentration of C–H, Schuster recognized that an E → V energy transfer following an exchange mechanism describes the experimental facts much better than a dipole–dipole energy transfer, since exchange transfer is independent of optical transition moments.

Exchange energy transfer between $^1O_2$ and solvent molecule can be initiated by repulsive interaction, which couples the highest frequency mode of the solvent with an electronic and vibronic transition of $^1O_2$. Equation 3 was given by Schuster for the

$$k_{XY} = Z \sum_{ms} F_m F_s R_{ms} \quad (3)$$

incremental rate constant k_{XY} if X–Y is the accepting oscillator of the solvent molecule. Here Z is a term independent of the specific nature of the solvent, F_m is the Franck–Condon (FC) factor for the $(^1\Delta_g, v = 0) \rightarrow (^3\Sigma_g^-, v = m)$ transition of O_2, F_s is the FC factor for the $(v = 0) \rightarrow (v = s)$ vibrational transition of the accepting oscillator X–Y, and R_{ms} is an off-resonance factor. Although no values for F_m, F_s, and R_{ms} have been given, Schuster qualitatively explained the decreasing quenching activity of oscillators X–Y in the series O–H > C–H > O–D > C–D by means of the respective energies E_{XY} of the highest fundamental vibrations. C–Cl, C–F, and C=S, however, did not fit into his explanation model and were omitted without further discussion.

With the $^1O_2$ lifetimes determined in this study new experimental material is now at hand completing previous data. We therefore calculate from our and literature data incremental rate constants k_{XY} in order to get more insight into the mechanism of radiationless deactivation of $^1O_2$ by solvent molecules.

For weakly deactivating solvents, like the ones we have investigated, radiative deactivation of $^1O_2$ by phosphorescence becomes important, as we found in $^1O_2$ phosphorescence quantum yield studies. Therefore k_D has to be calculated from eq 4, using

$$k_D = (1/\tau_\Delta - k_p)/[S] \quad (4)$$

the solvent-independent rate constant of phosphorescence of k_P = 7.1 s^{-1}, determined by us.[16,23]

After dividing the k_D values of solvents X_nY_m containing only one kind of vibrator by N_{XY}, the number of times the particular X–Y oscillator occurs per molecule, one obtains the k_{XY} values listed in Table III, which represent second-order rate constants

(18) Krasnovsky, A. A., Jr. *Chem. Phys. Lett.* **1981**, *81*, 443.
(19) Findlay, F. D.; Snelling, D. R. *J. Chem. Phys.* **1971**, *55*, 545.
(20) Penzhorn, R.-D.; Guesten, H.; Schurath, U.; Becker, K. H. *Environ. Sci. Technol.* **1974**, *8*, 907.
(21) Merkel, P. B.; Kearns, D. R. *J. Am. Chem. Soc.* **1972**, *94*, 7244.
(22) Salokhiddinov, K. I.; Byteva, I. M.; Gurinovich, G. P. *Zh. Prikl. Spektrosk.* **1981**, *34*, 892.
(23) We obtained for the radiative lifetime of $^1O_2$ in solution a mean value of 0.14 s, which is about 30 times smaller than Krasnovsky's value of 4.1 s.[18] This discrepancy will be discussed in ref 16.
(24) Leiss, A.; Schurath, U.; Becker, K. H.; Fink, E. H. *J. Photochem.* **1978**, *8*, 211.

Table III. Second-Order Rate Constants k_{XY} of Energy Transfer from $^1O_2$ to Oscillators X–Y[a]

X–Y	X_nY_m	k_D, M^{-1} s^{-1}	N_{XY}	k_{XY}, M^{-1} s^{-1}	ln k_{XY}	E_{XY}, cm^{-1}
O–H	OH_2	4290[13]	2	2145	7.67	3400
O–H	(CH_3OH)	3890[13]	(1)	2720	7.91	3340
C–H	C_6H_6	2840[13]	6	470	6.15	3050
C–H	$(CHCl_3)$	320[5]	(1)	320	5.77	3020
C–H	C_6H_{12}	4690[13]	12	390	5.97	2960
O–D	OD_2	330[13]	2	165	5.11	2500
O–D	(CD_3OD)	180[13]	(1)	156	5.05	2500
C–D	C_6D_6	140[13]	6	23	3.14	2290
C–D	$(CDCl_3)$	8.0	(1)	8.0	2.08	2250
C=S	CS_2	1.35	2	0.67	−0.39	1550
C–F	C_6F_6	3.84	6	0.64	−0.45	1520
C–F	C_6F_{14}	0.67	14	0.048	−3.04	1250
C–Cl	CCl_4	0.42	4	0.11	−2.25	850
S–H	SH_2 g	190[20]	2	95	4.55	2630
N–H	NH_3 g	2650[24]	3	900	6.80	3400

[a] N_{XY} = number of X–Y oscillators per solvent molecule X_nY_m, k_D = second-order rate constant of $^1O_2$ deactivation by X_nY_m, and E_{XY} = energy of highest frequency fundamental vibration of X–Y. The index g indicates gas-phase data.

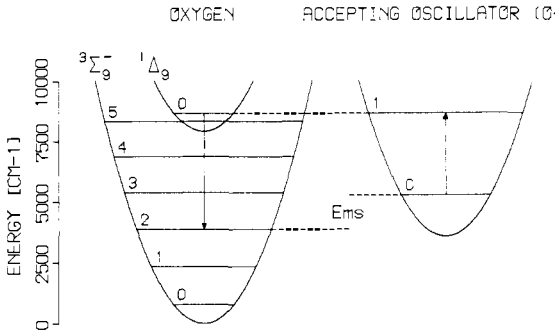

Figure 4. Schematic representation of the E → V energy-transfer channel from $^1O_2$ to the accepting oscillator O–H with $m = 2$ and $s = 1$. The energies of the different vibronic levels of the $^1\Delta_g$ and $^3\Sigma_g^-$ states have been taken from Herzberg.[25]

of energy transfer from $^1O_2$ to X–Y. For most oscillators more than one value is given. Some of the k_{XY} values are calculated from lifetime data of solvents containing two different vibrators, e.g., CH_3OH. In these cases from k_D the k_{XY} value with the lower E_{XY} is subtracted as many times as this X–Y vibrator is contained in the solvent molecule and afterward the difference is divided by N_{XY} of the high-energy oscillator. For these calculations the following k_{XY} values were used: $k_{CH} = 390$ and $k_{CD} = 8.0$ M^{-1} s^{-1}. In addition, gas-phase data for S–H and N–H are included in Table III.

From a comparison of the data it becomes obvious that there exists a strong and apparently linear correlation between ln k_{XY} and E_{XY}.

The question arises how the linear relation between the logarithmic rate constant of energy transfer from $^1O_2$ to an oscillator X–Y and its highest fundamental vibrational energy E_{XY} can be understood. For the interpretation we will discuss quantitatively the exchange energy-transfer model.

In our collisional model for the energy transfer from $^1O_2$ to an oscillator X–Y, several individual reaction channels are in competition, which are described by eq 5. Here m and s are the

$$O_2(^1\Delta_g, v = 0) + X\text{–}Y(v = 0) \xrightarrow{k_{XY}^{ms}} O_2(^3\Sigma_g^-, v = m) + X\text{–}Y(v = s) + E_{ms} \quad (5)$$

quantum numbers of the final vibronic states of O_2 and X–Y, and $E_{ms} = E_\Delta - (E_m + E_s)$ is the energy difference of the vibronic transitions or off-resonance energy of this particular reaction channel. Since E_{ms} has to be distributed over various vibrational (V), rotational (R), and translational (T) degrees of freedom of the whole solvent molecule the overall process is an E → V + R + T energy transfer. The rate constant k_{XY}^{ms} of the individual energy-transfer channel is expressed by eq 6.

Table IV. FC Factors F_m for $(^1\Delta_g, v = 0) \rightarrow (^3\Sigma_g^-, v = m)$ Transitions of O_2[26]

m				
0	1	2	3	4
9.87×10^{-1}	1.29×10^{-2}	1.36×10^{-4}	2.46×10^{-7}	2.5×10^{-10} [a]

[a] Extrapolated value with $\log F_m = -0.0393 - 1.535m - 0.2147m^2$.

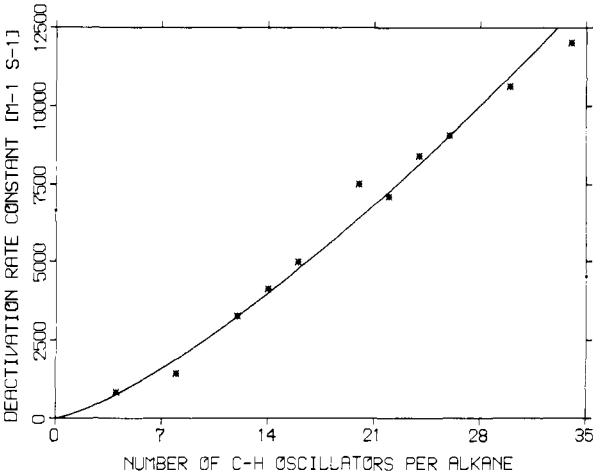

Figure 5. Second-order $^1O_2$ deactivation rate constant k_D of a series of alkanes C_nH_{2n+2} as a function of the number of C–H oscillators. Data from Rodgers[13] and Becker et al.[28]

$$k_{XY}^{ms} = ZF_mF_sR_{ms} \quad (6)$$

Figure 4 illustrates schematically the exothermic energy transfer to O–H as accepting oscillator with $m = 2$ and $s = 1$ according to eq 5. Of course, other energy-transfer channels are also possible, e.g., the almost resonant process with $m = 3$ and $s = 1$. The overall rate constant k_{XY} is given as the sum of the rate constants k_{XY}^{ms} of all possible individual energy-transfer channels; see eq 3.

Equations 3 and 6 will be used for the interpretation of the energy dependence of the k_{XY} values of Table III. Thus we have to discuss Z, F_m, F_s, and R_{ms} next.

Z is a constant including the probability of $^1\Delta_g \rightarrow {}^3\Sigma_g^-$ intersystem crossing. We suppose Z to be independent of oscillator X–Y in non heavy atom solvents.

FC factors F_m for the transitions of O_2 can be taken from the literature. They are listed in Table IV. The excitation probability of an overtone is much lower than the one of the fundamental vibration of X–Y. Since ln k_{XY} correlates linearly with the highest fundamental vibrational energy E_{XY} of the respective oscillator, only $v = 0 \rightarrow v = 1$ transitions will be considered. The energies of the $0 \rightarrow 1$ vibronic transitions of the X–Y oscillators of Table III are at least by a factor of 10 less than the corresponding dissociation energies in the electronic ground state. Therefore the model of a slightly distorted harmonic oscillator is a fairly good approximation for the fundamental transitions of all these oscillators. Consequently, we expect the FC factors F_s for the $0 \rightarrow 1$ transitions of the X–Y listed in Table III to be approximately the same.

The dependence of the energy-transfer probability on E_{ms} can be expressed by the off-resonance factor R_{ms}, whereby the exact form of $R_{ms} = f(E_{ms})$ is not known. Since the excess energy E_{ms} can be accepted by a large number of different vibrational and rotational modes and partially be transferred into translational energy, the calculation of $R_{ms} = f(E_{ms})$ is too complex in the case of a polyatomic acceptor molecule. However, for the much easier E → V + T energy transfer from excited mercury to a diatomic

(25) Herzberg, G. *Spectra of Diatomic Molecules*; Van Nostrand Reinhold: New York, 1950; p 560.
(26) Halmann, M.; Laulicht, I. *J. Chem. Phys.* **1965**, *43*, 438.

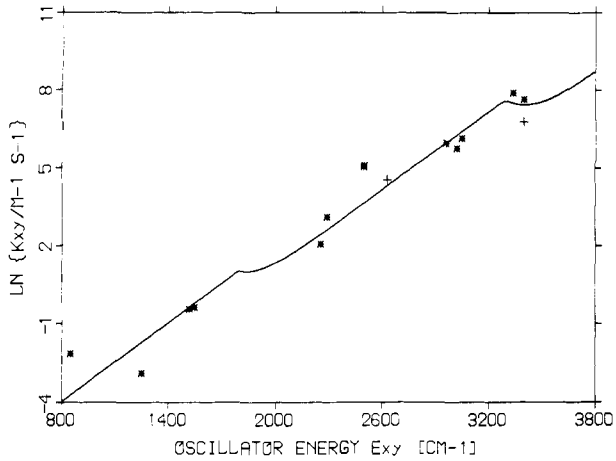

Figure 6. Dependence of the logarithmic incremental rate constant k_{XY} of $^1O_2$ deactivation on the highest fundamental oscillator energy E_{XY}: (*) data from liquid phase; (+) data from gas phase (see Table III). Curve best fit according to eq 9.

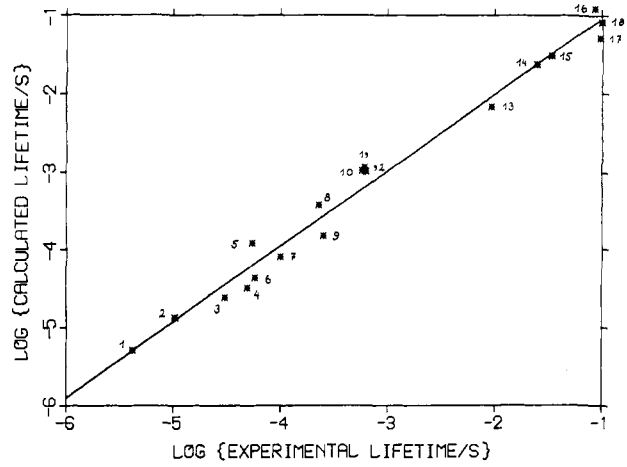

Figure 7. Double-logarithmic plot of calculated vs experimental $^1O_2$ lifetimes for various solvents. Calculation occurred using E_{XY} literature data and fit of Figure 6. Maximum deviation of calculated τ_Δ from experimental τ_Δ: factor of 2. Lifetime data[4,5,13] and from Table I. Linear least-squares fit: slope = 0.97, intercept = −0.06, correlation coefficient 0.99. Numbers indicate solvents: (1) H_2O, (2) CH_3OH, (3) C_6H_6, (4) acetone-h_6, (5) D_2O, (6) CH_3CN, (7) CH_2Cl_2, (8) CD_3OD, (9) $CHCl_3$, (10) acetone-d_6, (11) CD_3CN, (12) C_6D_6, (13) $CDCl_3$, (14) C_6F_6, (15) CS_2, (16) CCl_4, (17) C_6F_{14}, and (18) $C_2F_3Cl_3$.

acceptor molecule, Dickens et al. calculated the dependence of R_{ms} on E_{ms} to be approximately exponential.[27] We adopt this result and approximate R_{ms} ($s = 1$) by eq 7, with α being assumed

$$R_{ms} = e^{-\alpha E_{ms}} \tag{7}$$

to be independent of solvent nature. In a more exact treatment α would depend on solvent molecular structure and probably on the nature of X–Y, too. This follows from the positive curvature of the plot of k_D values against the number of C–H oscillators of a series of alkanes given in Figure 5. Since the possibility of distribution E_{ms} over different vibrational and rotational modes increases with increasing N_{CH}, R_{ms} becomes larger and k_D grows stronger than linear with N_{CH} for small N_{CH} values. Consequently, α is a measure for the ability of the solvent molecule to accept E_{ms}. With increasing number of vibrational and rotational modes α becomes smaller.

Equation 7 holds for exothermic processes as shown for example in Figure 4. $R_{ms} = 1$ in the case of resonant energy transfer. In the case of endothermic energy-transfer channels ($E_{ms} < 0$; e.g., $m = 3$, $s = 1$ in Figure 4), we calculate R_{ms} by eq 8.

$$R_{ms} = e^{E_{ms}/RT} \tag{8}$$

Thus, taking together Z and F_s ($s = 1$) in the constant K, we find k_{XY} is given by

$$k_{XY} = K\sum_m F_m R_{ms} \tag{9}$$

With the FC factors of Table IV, the best description of the experimental data by eq 9 is obtained in a two-parameter fit with $K = 6.4 \times 10^9$ M^{-1} s^{-1} and $\alpha = 5 \times 10^{-3}$ cm. The calculated curve is shown in Figure 6 together with the experimental data.

Considering its approximative character, eq 9 describes remarkably well the dependence of the rate constant of energy transfer from $^1O_2$ to an accepting oscillator X–Y on its highest vibrational 0–1 transition energy. Obviously, the experimentally observed exponential relationship between k_{XY} and E_{XY} is reproduced by our energy-transfer model.

There are two shoulders at about 1800 and 3300 cm^{-1}, which interrupt the linear correlation of ln k_{XY} with E_{XY}. Both steps result from the graduation of the FC factors for the $0 \rightarrow m$ transitions of O_2 given in Table IV. The step at 1800 cm^{-1} would be more pronounced if the FC factor for the $0 \rightarrow 4$ transition would be larger than 2.5×10^{-10} and would vanish if it would be less than 2×10^{-11}. Similar considerations hold true for the shoulder at 3300 cm^{-1}.

The vibrational excitation distribution of $O_2(^3\Sigma_g^-)$ depends on the excitation energy E_{XY} of oscillator X–Y. For example, the analysis of the individual rate constants k_{XY}^{ms} for the energy transfer from $^1O_2$ to OH demonstrates that besides $v = 1$ excited O–H, 2% of the $O_2(^3\Sigma_g^-)$ is formed in $v = 1$, 45% in $v = 2$, and 53% in $v = 3$.

On the other hand, with O–D as accepting vibrator, 1% of $O_2(^3\Sigma_g^-)$ is produced in $v = 1$, 22% in $v = 2$, and 77% in $v = 3$.

Our finding that initially in $^1O_2$ deactivation by solvent molecules a vibrationally hot ground-state oxygen ($v = 2$, 3) is produced agrees with the results on $^1O_2$ ($^1\Delta_g$, $v = 0$) deactivation by $O_2(^3\Sigma_g^-)$ obtained by Maier et al.[29] These authors found that in liquid O_2 the major deactivation channels also lead to the formation of $^3\Sigma_g^-$ $v = 2$ and $v = 3$ molecules.

In solution further deactivation of the primary vibrationally excited energy-transfer products occurs probably very rapidly. O_2 will lose its energy by subsequent V → V energy-transfer processes with solvent molecules via energetically suitable oscillators and X–Y will disperse its energy over the large number of vibrational and rotational degrees of freedom of the corresponding solvent molecule, which for large molecules requires only about 10 ps[30].

The same $^1O_2$ deactivation mechanism that is effective in the liquid phase also operates in the gas phase. This is demonstrated by the accordance of the data of Table II and by the satisfying inclusion of gas-phase data into the plot of Figure 6.

The large deuterium isotope effect on $^1O_2$ lifetimes ($CHCl_3$, $\tau_\Delta = 250$ μs; $CDCl_3$, $\tau_\Delta = 9400$ μs) is easily and quantitatively understood by the plot of Figure 6. The C–D oscillator energy is about 750 cm^{-1} lower and thus the off-resonance energy is about 750 cm^{-1} larger for perdeuteriated hydrocarbons than the respective values in hydrocarbons. Since the slope amounts to $\alpha = 0.005$ cm, this results in a 40-fold lower energy-transfer probability.

The energy-transfer model for $^1O_2$ deactivation presented here is based essentially on exothermic processes. Endothermic energy-transfer channels play only a minor role. Therefore it is not unexpected that even in solvents with long $^1O_2$ lifetimes τ_Δ values are only very weakly temperature dependent.

A. Calculated versus Experimental Lifetimes. By means of eq 10 and $k_P = 7.1$ s^{-1} it is possible to calculate from incremental rate constants $^1O_2$ lifetimes in solution. Although the k_{XY} values

$$\tau_\Delta = (k_P + [S]\sum_{XY} N_{XY} k_{XY})^{-1} \tag{10}$$

(27) Dickens, P. G.; Linnett, J. W.; Sovers, O. *Discuss. Faraday Soc.* **1962**, *33*, 52.
(28) Becker, K. H.; Groth, W.; Schurath, U. *Chem. Phys. Lett.* **1971**, *8*, 259.
(29) Wild, E.; Klingshirn, H.; Maier, M. *J. Photochem.* **1984**, *25*, 131.
(30) Gottfried, N. H.; Seilmeier, A.; Kaiser, W. *Chem. Phys. Lett.* **1984**, *111*, 326.

of Table III give a much closer correlation with experimentally determined τ_Δ values, since they are derived from them, we evaluate fitted k_{XY} rate constants for the calculation of τ_Δ from the curve of Figure 6, using literature data for the highest fundamental vibrational energies of oscillators X–Y (see, for example, Table III). By comparing τ_Δ values calculated in this way with experimental values, it then becomes obvious to which extent the energy-transfer model used by us for the description of the E_{XY} dependence of k_{XY} reproduces realistic $^1O_2$ lifetimes in solution.

Figure 7 illustrates in a double-logarithmic plot the excellent correlation between calculated and experimental values. A linear least-squares fit of the data results in a straight line with slope 0.97 and intercept −0.06.

Thus the energy-transfer model proposed by us quantitatively describes the solvent dependence of the $^1O_2$ lifetime in solution. Since collisional deactivation of $^1O_2$ can occur in the gas phase and in polymers, too, our correlation may also be used for calculating lifetimes in these phases.

Conclusion

Deactivation of $^1O_2$ by solvent molecules is a collisional E → V + R + T energy transfer, which occurs by coupling of the highest fundamental vibrational mode X–Y of the acceptor molecule with an O_2 ($^1\Delta_g$, $v = 0$) → ($^3\Sigma_g^-$, $v = m$) transition. The off-resonance energy E_{ms}, which is the energy difference of the vibronic transitions in O_2 and the accepting oscillator X–Y, has to be accepted simultaneously by various other vibrational and rotational modes of the solvent molecule.

The increase of energy-transfer rate constant k_{XY} with vibrational energy E_{XY} of the highest 0 → 1 transition of oscillator X–Y is qualitatively explained by the reduction of the off-resonance energy to the various 0 → m transitions of O_2.

Quantitatively the dependence of k_{XY} on E_{XY} is given by eq 9 using an exponential correlation between off-resonance factor R_{ms} and off-resonance energy E_{ms} (eq 7).

Thus we present an energy-transfer model for the $^1O_2$ deactivation by solvent molecules which for the first time gives a reasonable physical understanding of this process *and* describes quantitatively the solvent dependence of $^1O_2$ lifetimes over more than 4 orders of magnitude.

Acknowledgment. We gratefully acknowledge financial support from the Deutsche Forschungsgemeinschaft and the Fonds der Chemischen Industrie.

Registry No. O_2, 7782-44-7; C_6F_{14}, 355-42-0; C_6F_6, 392-56-3; $CFCl_3$, 75-69-4; $C_2F_3Cl_3$, 76-13-1; CCl_4, 56-23-5; CS_2, 75-15-0; $CDCl_3$, 865-49-6.

Mechanism of Spin-State Interconversion in Ferrous Spin-Crossover Complexes: Direct Evidence for Quantum Mechanical Tunneling

Chuan-Liang Xie and David N. Hendrickson*

Contribution from the School of Chemical Sciences, University of Illinois, Urbana, Illinois 61801. *Received March 19, 1987*

Abstract: The pulsed-laser photolysis technique is used to monitor in the 300 to 4.2 K range the relaxation from the high-spin state ($^5T_2$) to the low-spin ground state ($^1A_1$) of the Fe^{II} spin-crossover complex $[Fe(6\text{-Me-py})_2(py)tren](ClO_4)_2$ doped in polystyrene sulfonate (PSS). The hexadentate ligand $(6\text{-Me-py})_2(py)tren$ is the Schiff base condensate from the reaction of 2 mol of 6-methyl-2-pyridinecarboxaldehyde, 1 mol of 2-pyridinecarboxaldehyde, and 1 mol of tris(2-aminoethyl)amine (tren). Mössbauer data for a ^{57}Fe-enriched sample of the PSS-doped complex establish that at temperatures below 340 K all of the complexes are in the low-spin state. An excitation profile obtained by monitoring the change in the electronic absorption spectrum at several different wavelengths after a single pulse of the Q-switched Nd/YAG laser establishes the fact that the phenomenon is a $^5T_2 \rightarrow {}^1A_1$ spin-crossover relaxation. At temperatures below ~120 K the relaxation rate (k) becomes relatively independent of temperature with a value of 1.4 (± 0.5) × 10^5 s^{-1} in the 50–4.2 K range. The temperature independence of the rate is direct evidence of quantum mechanical tunneling. Above ~140 K an Arrhenius plot of ln k vs. $1/T$ gives a straight line with a slope of 823 cm^{-1}. By fitting all of the 300–4.2 K relaxation rate data for the PSS-doped complex to two different theoretical models, it is shown that not only is quantum mechanical tunneling dominant at temperatures below ~120 K, but tunneling is also the predominant mechanism by which the complex makes a spin-state interconversion in the 140 to 300 K range.

Spin-crossover complexes have been reported for several different transition metals; however, those of Fe^{II} and Fe^{III} have been studied the most.[1-5] The factors which control the bulk properties (i.e., discontinuous vs. gradual) of the spin-crossover transformation in the solid state have been the main focus. On the other hand, not as much attention has been directed at understanding the dynamics and mechanism of the spin-state interconversion process. One of the reasons for this is the lack of experimental techniques which can be used to monitor directly the spin-state interconversion process in the solid state. Techniques such as Mössbauer, FTIR, and EPR spectroscopies have been used; however, the time-scale window associated with each of these techniques is very narrow. Only in the very few cases where the spin-state interconversion rate in the solid state is close to the time scale associated with a particular physical technique has it proven possible to obtain kinetic information from line-broadening studies.[6] For example, Maeda et al.[7] have very recently identified

(1) Gütlich, P. In *Structure and Bonding*; Spinger-Verlag: Berlin, 1981; Vol. 44, p 83.
(2) König, E.; Ritter, G.; Kulshreshtha, S. K. *Chem. Rev.* **1985**, *85*, 219–234.
(3) Rao, C. N. R. *Int. Rev. Phys. Chem.* **1985**, *4*, 19–38.
(4) Gütlich, P. In *Mössbauer Spectroscopy Applied to Inorganic Chemistry*; Long, G. J., Ed.; Plenum Press: New York, 1984.
(5) Gütlich, P. In *Chemical Mössbauer Spectroscopy*; Herber, R. H., Ed.; Plenum Press: New York, 1984.
(6) Goldanskii, V. I. *Pure Appl. Chem.* **1983**, *55*, 11.
(7) (a) Maeda, Y.; Tsutsumi, N.; Takashima, Y. *Inorg. Chem.* **1984**, *23*, 2440–2447. (b) Maeda, Y.; Oshio, H.; Takashima, Y.; Mikuriya, M.; Hidaka, M. *Ibid.* **1986**, *25*, 2958–2962. (c) Maeda, Y.; Takashima, Y.; Natsumoto, N.; Okyoshi, A. *J. Chem. Soc., Dalton Trans.* **1986**, 1115. (d) Matsumoto, N.; Ohta, S.; Yoshimura, C.; Ohyoshi, A.; Kohata, S.; Okawa, H.; Maeda, Y. *Ibid.* **1985**, 2575.

0002-7863/87/1509-6981$01.50/0